ELSEVIER

Coordination Chemistry Reviews
222 (2001) 127–154

COORDINATION CHEMISTRY REVIEWS

www.elsevier.com/locate/ccr

Macrocyclic polyethers as probes to assess and understand alkali metal cation-π interactions

George W. Gokel [a,*], Leonard J. Barbour [b], Stephen L. De Wall [a], Eric S. Meadows [a]

[a] *Bioorganic Chemistry Program, Department of Molecular Biology and Pharmacology, Washington University School of Medicine, 660 South Euclid Avenue, Campus Box 8103, St. Louis, MO 63110, USA*

[b] *Department of Chemistry, University of Missouri, 601 S. College Avenue, Columbia, MO 65211, USA*

Received 2 January 2001; received in revised form 12 March 2001; accepted 12 March 2001

Contents

* Corresponding author. Tel.: +1-314-362-9297; fax: +1-314-362-9298.
E-mail address: ggokel@molecool.wustl.edu (G.W. Gokel).

PII: S0010-8545(01)00380-0

Abstract

Cation-π interactions of alkali metals with arenes have been known in the gas phase for two decades but solid-state structural data have become available only recently. The quest for solid-state evidence is described here. Complexation of Na^+ and K^+ by arene-terminated lariat ethers has provided important insights into the cation-π interaction.

Keywords: Alkali metal; Arene; Cation-π interaction; Host–guest; Crown ether; Lariat ether

1. Introduction

A number of alkali metal, alkaline earth metal, and transition metal ions are important to living organisms. Among these, the most abundant are sodium, potassium, and calcium. Potassium cation, for example, is present inside red blood cells at a concentration of about 150 mM. Sodium is present within red blood cells at a much lower concentration but externally in plasma its concentration is about 150 mM. The high concentrations of these metals in natural systems encourage the study of their interactions with natural donor groups.

A significant problem in the analysis of alkali metal cations is the fact that they are essentially featureless spheres. The alkali metals (lithium, sodium, potassium, rubidium, cesium, and francium) all preferentially form cations having a single positive charge. Because the monovalent ions differ in size, they exhibit decreasing Lewis acidity from lithium to francium. Sodium cation is about 2 Å in diameter and the diameter of K^+ is about 2.7 Å. By comparing their sizes, we conclude that the potassium cation is only about 50% as 'charge dense' as is sodium cation. Another way of expressing this concept is that Na^+ is a stronger Lewis acid than is K^+. Apart from the physical size and the resulting difference in charge density, however, there is little to differentiate the two cations.

The study of alkali metal cations was advanced immensely by Pedersen's discovery of macrocyclic 'crown' polyethers [1] and Lehn's invention of the cryptands [2]. As a result, complexes of many alkali metal cations could be prepared, characterized, and studied. Structural variations designed into the crowns and cryptands permitted a study of the influence of donor groups on the binding interactions [3]. So important was the development of these novel compounds that they were recognized with the award of the 1987 Nobel Prize in Chemistry.

The importance of alkali metal chemistry relates to the prominence of these cations in nature. Alkali metal cations can serve as counterions for such amino acids as aspartic and glutamic acids in which the sidechains are CH_2COOH and CH_2CH_2COOH, respectively. Alkoxides are unlikely to form from the hydroxyl sidechains of serine or threonine because the pH in biological systems is too near neutrality. It is possible that tyrosine's phenolic hydroxyl group could ionize and become associated with an alkali metal cation. These are clearly the major interactions that have been considered historically.

In recent years, the possibility of cation-π interactions with the sidearms of the amino acids phenylalanine (Phe, F), tyrosine (Tyr, Y), and tryptophan (Trp, W) has proved intriguing and has provoked considerable speculation. It was proposed, for example, that K^+–arene interactions might play a critical role in determining the selectivity of potassium protein channels [4]. This postulate failed to stand up to an experimental test [5] but stimulated considerable interest in the subject of cation-π interactions.

During recent years, evidence for cation-π interactions has come largely from two sources: mass spectrometry and calculations. Pioneering mass spectrometric studies were reported in 1981 by Sunner, Nishizawa, and Kebarle [6]. They found that the enthalpy of interaction between benzene and K^+ was significant and similar to the interaction of K^+ with either methanol or water. Castleman and coworkers conducted similar mass spectrometric experiments with Na^+ [7]. Because sodium cation is more charge dense than K^+, the enthalpies of interaction between Na^+ and benzene were greater than for K^+ and benzene. Likewise, the variation in the energies of interaction between Na^+ and either water or methanol was larger than the corresponding interaction with K^+. Still, the interactions between Na^+ and all three oxygen-donor species exhibited similar strengths. Lisy and coworkers have reported additional computational and mass spectrometric evidence of alkali metal–arene cation-π interactions [8]. The presumed K^+–benzene interaction is shown schematically in Fig. 1.

A few X-ray crystal structures have been reported that suggest cation-π interactions involving alkali metal cations [9]. Two structures that have been available for a number of years deserve special note. The first is the structure of $K^+B(C_6H_5)_4^-$ [10]. It is shown in Fig. 2 in a top view (top). Potassium is nestled between two of the four benzene rings. The $K^+\cdots$arene distance is ca. 3.0 Å. If the thickness of a benzene ring is 3.4 Å and the radius of K^+ is 1.33 Å, then the contact distance should be 3.03 Å or essentially the value that is observed. Interestingly, the 3rd and 4th benzenes of the anion cradle an adjacent K^+ (not shown). Likewise, the K^+ that is shown is cradled by two the benzenes of an adjacent anion. Thus, in the solid-state, each K^+ is effectively 'bound' by four benzenes. The result in the crystal lattice is an extended column that alternates between an anion and a cation. Of

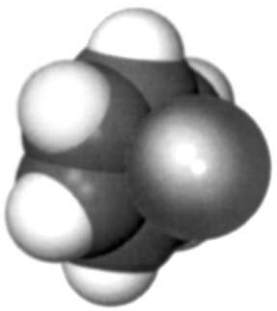

Fig. 1. Schematic of the interaction between K^+ and benzene in the gas phase.

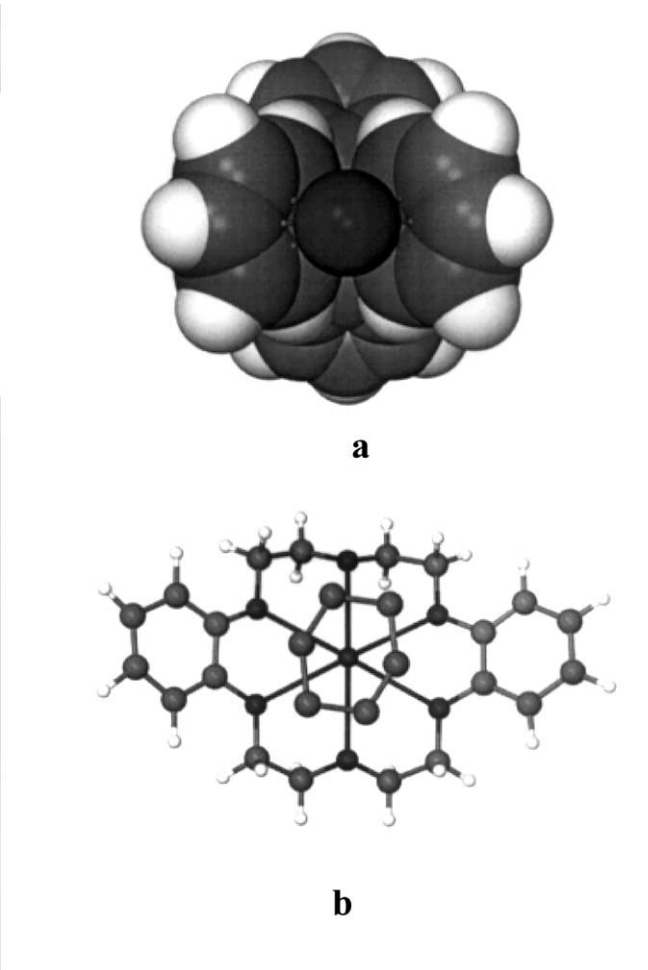

Fig. 2. X-ray crystal structure of $KB(C_6H_5)_4$ (top view, top panel) and structure of dibenzo-18-crown-6 · K · benzene complex (top view, bottom panel).

course, it could be argued that there would otherwise be a void between the aromatic rings and K^+ is filling space rather than being complexed by benzene. In other words, the cation's position is as close to the negative charge on boron as possible within the existing structural framework.

In 1981 Hrncir et al. [11] reported an X-ray structure of dibenzo-18-crown-6. In this structure, K^+ was bound by the macrocycle but it was centered about 0.3 Å above the mean plane of the donor groups. The displacement of the cation was towards a benzene ring that occupied the apical position. The structure is shown in a top view in Fig. 2, panel b. Beyond these two structures, however, solid-state evidence was limited.

In the early 1980s, we became intrigued by the question of cation-π interactions and focused our attention on olefins and alkynes as potential donors. We devised an experimental system based on the compounds we had named lariat ethers [12]. Before elaborating further our effort to obtain experimental evidence for cation-π interactions, some discussion is in order for crown and lariat ether compounds.

2. Crown ethers and cryptands

Crown ethers are now well-known molecules. They are characterized by repeating (CH_2CH_2O) units. The simplest examples are unfettered by substituents and can be fully described as $(CH_2CH_2O)_n$. The most common simple macrocycle is 18-crown-6, which has the formula $(CH_2CH_2O)_6$. The crown of this type that has been known the longest is actually 12-crown-4 [$(CH_2CH_2O)_4$], which was patented in 1957 [13]. The full promise of these compounds remained unrealized until 1967 when Pedersen disclosed the preparation of dibenzo-18-crown-6 and demonstrated its ability to complex alkali metal cations. The structures of 12-crown-4, 15-crown-5, and 18-crown-6 are shown along with the reaction of dibenzo-18-crown-6 with KCl (Fig. 3).

The cryptands are related to crown ethers but were developed to be three-dimensionally enveloping cation-complexing agents. Like the crown ethers, they are characterized by (CH_2CH_2O) units. They differ in that a third strand bridges the crown-like macrocycle. Typically, the third strand is attached to the macrocycle at nitrogen atoms that replace two of the oxygens of the crown. Thus, the compound known as [2.2.2]cryptand has three ($CH_2CH_2OCH_2CH_2OCH_2CH_2$) strands, each of which is connected to nitrogen. Numerous structural variations are possible in cryptand structures as they are for crown ethers. Indeed, by the 1980s, literally thousands of crown ethers and cryptands were known [14].

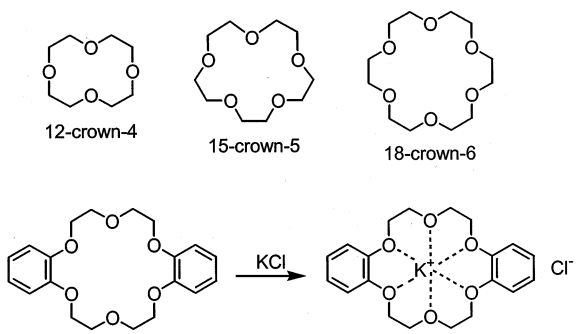

Fig. 3. Structural formulas of 12-crown-4, 15-crown-5, 18-crown-6, and dibenzo-18-crown-6, the latter complexing KCl.

2.1. Lariat ethers

Crown ethers and cryptands complex alkali metal cations. One difference is that cryptands typically exhibit greater cation selectivity but crowns exhibit faster cation binding dynamics. The latter was of interest to us because natural ionophores exhibit both fast binding rates and good cation selectivities. An example is valinomycin, a well-studied cyclododecadepsipeptide. It is a 36-membered ring comprised of amino- and hydroxyacids that selectively binds K^+ over Na^+. Moreover, it transports K^+ very effectively in vivo (Fig. 4).

Valinomycin forms a three-dimensional, cryptand-like complex with K^+. In the unbound state, it is a macrocycle like the crown ether. It achieves three-dimensionality by folding over the K^+ in a 'tennis ball seam' arrangement. This is possible because the macrocycle is relatively large and because the conformation it adopts is facilitated by its unusual $(D,D,L,L,)_3$ stereochemistry.

Lariat ethers were designed in an effort to mimic the binding and selectivity properties of valinomycin. We recognized that three-dimensional complexation would be required in order to isolate a cation from the surrounding medium and thus achieve good binding strength and selectivity. The question of binding dynamics could be understood in a more quantitative way. The complexation reaction between a 'host' or 'receptor' molecule and a cationic guest can be expressed by the following equilibrium relationship.

$$\text{receptor} + \text{cation} \underset{k_{\text{release}}(k_{-1})}{\overset{k_{\text{complex}}(k_1)}{\rightleftharpoons}} \text{complex} \tag{1}$$

The complexation rate constant in the equation shown (Eq. (1)) is k_{complex}, (also referred to as k_1 or k_f for forward rate). The rate at which the cation (guest) is released is k_{release} ($k_{\text{decomplex}}$, k_{-1}, or k_{backward}). The cation binding selectivity is expressed as their ratio, $K_S = k_1/k_{-1}$, i.e. $K_S = k_{\text{forward}}/k_{\text{release}}$.The rate at which

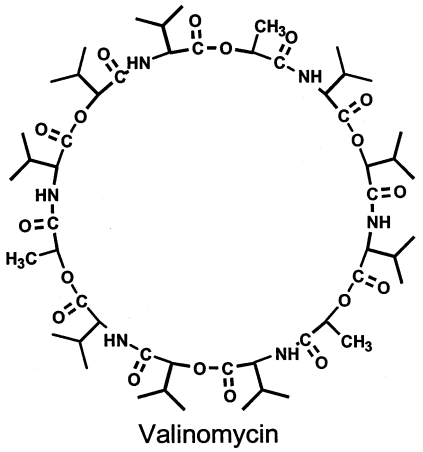

Fig. 4. Structural formula of vlinomycin.

cations are bound and released by the receptor molecule is defined by the individual rates. A compound that binds and releases quickly would have good binding dynamics but could exhibit poor equilibrium stability constant. For example, if $k_1 = 10^8\ \mathrm{M}^{-1}\,\mathrm{s}^{-1}$ and $k_{-1} = 10^7\ \mathrm{s}^{-1}$, the ratio, $\log K_S = 10^8/10^7 = 10\ \mathrm{M}^{-1}$. A compound having poor binding dynamics could still be a powerful binder. Thus a ratio of $10^5\ \mathrm{M}^{-1}\,\mathrm{s}^{-1}/10^1\ \mathrm{s}^{-1} = 10^4$ or $10\,000\ \mathrm{M}^{-1}$. The advantage of the high binding constant in the static sense is offset by the poor cation release dynamics.

Cation complexation rates for crown ethers are generally fast because crowns are essentially two-dimensional and access to the macrocycle from 'above' and 'below' is relatively unobstructed [15]. Decomplexation of the cation is likewise facile because the cation complex is unencumbered in the apical positions except by solvent or the counterion. Decomplexation involves solvent replacement of the cation within the macrocycle. For crown ethers, solvent is typically already in contact with the cation on either one or both sides of the complex. Crown complexation of cations is thus a dynamic process. This is favorable if the desired use of the receptor is as an ionophore e.g. a transmembrane carrier. Typically, cation selectivities for crowns are less impressive than they are for cryptands [16]. However, the very three-dimensionality and rigidity that confers remarkable cation selectivity on cryptands exacts a significant cost in binding and release dynamics.

Carrier-mediated transmembrane transport involves three 'stages'. This can be expressed by the use of the simple diagram shown in Fig. 5. The dark 'ring' represents a receptor compound such as valinomycin or a crown ether. The cation is initially present in the 'source phase' shown at the left of the diagram. The receptor molecule is dissolved in the membrane, which may be a bulk organic phase or a phospholipid bilayer separating the two aqueous phases. When the receptor and cation are in proximity at the phase boundary, a complex is formed. The complex then diffuses across the membrane layer to the opposite interface. When the complex approaches the phase boundary, solvent competes for the bound cation, which is decomplexed or released into the receiving phase. It should be

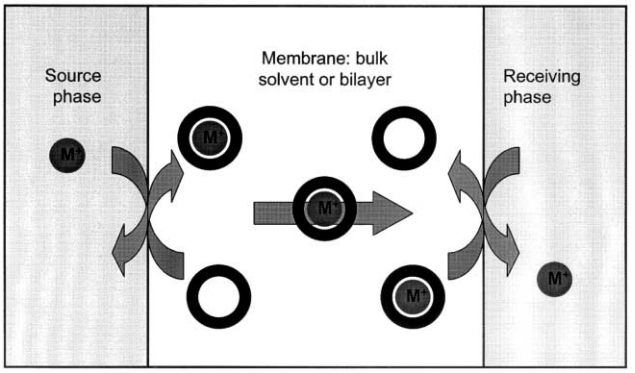

Fig. 5. Schematic diagram showing the major features of carrier-mediated transmembrane cation transport.

clearly understood that the diagram shown is an aid to conceptualization and is over-simplified. Cation transport and transmembrane conveyance of a cation is a multi-step process [17].

Ideally, one wants to have fast binding, fast release, and strong complexation strength within the membrane. Because K_S is the ratio k_1/k_{-1}, high values of all three are not simultaneously possible. Thus, compromises must be made. Complexation rate constants, because they typically involve very fast kinetics, are more difficult to obtain than equilibrium stability constants. Some data are available and are summarized in Table 1. Ideally, one would like all data to be available in water. Failing that, a uniform compromise solvent would be desirable. The requirement of solubility for both the receptor molecule and the salt has made methanol a favored, but not exclusive, solvent for these studies. Methanol is less polar than water and, generally, complexation and decomplexation rates are faster and binding is stronger in methanol than in water. Regrettably, the data shown in Table 1 were not determined in the same solvent but, to our knowledge, the comparison is the best currently available.

The development of lariat ethers [18] was intended to capitalize on the concept of flexibility to incorporate both the binding dynamics of crown ethers and the three-dimensional enveloping interactions known for cryptands and for valinomycin. The design used a simple crown macroring to impart to the system a rudimentary 'hole size' selectivity while retaining binding dynamics. Attachment of one or more sidearms that incorporated donor groups was expected to provide the third dimension of cation–donor interaction. As shown below in the scheme, the process was expected to involve two steps. Ultimately, excellent studies conducted by Eyring, Petrucci and their coworkers confirmed the kinetically distinct steps (Fig. 6).

In the first step, the cation is bound by the macroring to form a typical crown ether complex. A conformational change, a process that is typically rapid, affords the secondary, three-dimensional complexation interaction. The first step might be described as 'roping' the cation and the second as tying it up. In addition, molecular models of crowns having the types of sidearms used in the lariat ethers resemble a looped rope or lariat. The combination of the appearance and the concept led to the name 'lariat ether'.

Table 1
Rate and equilibrium constants for 18-crown-6 and [2.2.2]cryptand

Compound	$k_{complex}$ ($M^{-1}\,s^{-1}$)	$k_{release}$ (s^{-1})	K_S (M^{-1})
18-Crown-6 [a]	4.3×10^8	3.7×10^6	115
[2.2.2]Cryptand [b]	7.5×10^6	38	2×10^5

[a] Data for H_2O.
[b] Data for methanol solution.

2.1.1. Classes of lariat ethers

Once the basic notion of adding a flexible sidearm to a macrocycle was formulated, questions of ring size, sidearm identity, sidearm length, and numerous other variables had to be addressed. Foremost among these, it seemed to us, was the question of how the sidearm would be attached, as this would directly affect the dynamics, and ultimately the selectivity of the system.

The basic unit of the lariat ether was to be a crown ether. Crown ethers are defined by the presence of ethyleneoxy[–(CH_2CH_2O)–$_n$] units so any sidearm that was incorporated would require attachment in a limited number of ways. For an all-oxygen crown, the sidearm could be attached only to a carbon atom because trivalent oxygen would be unstable. Attachment of the sidearm on carbon introduces the issue of 'sidedness'. Since carbon is tetrahedral, potentially chiral, and noninvertable, approach of the cation to the crown from the side opposite would be more favorable. Conversely, approach from the sidearm-substituted side would be unfavorable. The latter could lead to decreased binding dynamics.

Despite the anticipated difficulties, some molecules were prepared in which the sidearm was attached to macroring carbon [19]. Cation complexation studies clearly showed that appropriate sidearm interactions enhanced cooperation between the macroring and the sidearm and thus binding strength. Even so, binding enhancements were not very significant compared to compounds having sidearms that lacked additional donors. A number of other research groups have elaborated the 'carbon-pivot' structures with considerable success [20].

In contrast, our efforts have focused largely on compounds in which one or more sidearms are attached at a macroring nitrogen atom. We termed these compounds 'nitrogen-pivot' lariat ethers. They proved to be relatively flexible, achiral, and synthetically accessible. As studies progressed, lariat ethers were prepared that possessed two or three sidearms. Using the Latin word *bracchium* for arm, we termed them 'bibracchial lariat ethers' (BiBLEs) or 'tribracchial lariat ethers' (TriBLEs). Examples of one-, two-, and three-armed lariat ethers are shown in Fig. 7.

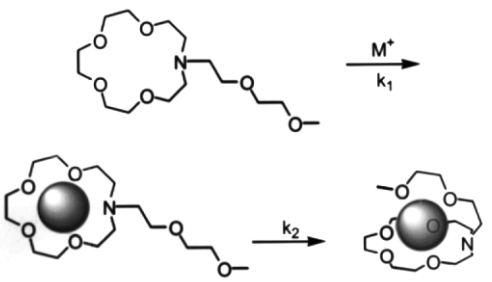

Fig. 6. Schematic of two-step cation complexation by lariat ethers.

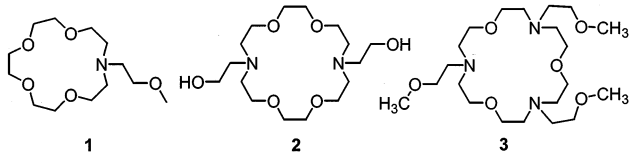

Fig. 7. Structures of **1**–**3**.

2.2. The quest for cation-π interactions

When the studies reported here commenced, some experimental evidence was in hand concerning cation-π interactions. As noted above, gas phase data were available and two suggestive crystal structures had been reported. Inferential evidence concerning related cations was also available. For example, the interaction of silver cations with π-bonds had been demonstrated by solid-state structural studies and by NMR methods [21]. The use of silver impregnated supports in gas chromatographic columns was well-established [22]. The type of clear experimental evidence that we sought was scarce.

It should be clearly stated that theoretical studies of alkali metal cation-π interactions have been undertaken and reported. In particular, these have been reported for a variety of arenes. Such calculations generally support the possibility of cation-π interactions [4,23]. Particular attention has been paid to benzene, phenol, and indole because they are present in the sidechains of phenylalanine, tyrosine, and tryptophan. Likewise, the cations Na^+ or K^+ have been of special interest because they are so common in biological systems. Burley and Petsko [24] have analyzed data available in the Protein Data Bank in an effort to identify ammonium cation-π interactions. They identified a number of close contacts between benzene and such residues as protonated lysine ($-NH_3^+$). A combination of theoretical and experimental studies has produced information about ammonium ion–arene interactions [25,26].

Our early interest was in the possible interaction of alkali metal ions with double and triple bonds. Admittedly, the naturally occurring amino acids do not possess alkenyl or alkynyl sidechains but their simplicity commended them.

Our plan was to use bibracchial (two-armed) lariat ethers to study alkali metal to olefin interactions. We felt that the crown would provide stabilization for the alkali metal cation in the form of a traditional equatorial complex. In principle, this should leave exposed the apical positions. Donor groups such as double or triple bonds on the flexible sidearms could then be positioned for apical interaction with the cation. Such an interaction would be required to compete with the counter anion. Although the ultimate goal was to obtain solid-state structural evidence, if the cation-π interactions were reasonably strong, they should be detectable by a variety of methods. Indeed, evidence of cation-π interactions in solution would be welcome and exciting.

4,13-Diaza-18-crown-6 was chosen as the basic experimental vehicle for these studies. The 18-membered ring forms symmetrical complexes with potassium and

many solid-state structures of them are available. The 15-membered analogs have the advantage that they offer a better macroring fit for Na^+, which is more charge dense than K^+. The 15-membered ring compounds are more difficult to synthesize and fewer complexes have been prepared. Whether the dearth of data reflected fewer attempts or poorer prospects was unknown as the effort commenced. The compounds selected for the studies described here are shown below as compounds **4**–**11**. The sidearms are: *n*-propyl, **4**, [27]; allyl, **5**, [23]; propargyl, **6**, [23]; cyanomethyl, **7**, [28]; benzyl, **8**, [23,29]; phenethyl, **9**; hydroxyphenethyl, **10**, [30]; and indolylethyl, **11**, [31].

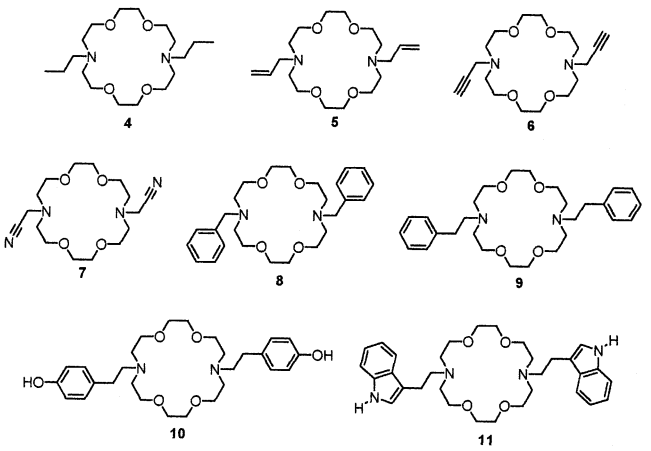

We had developed two different methods for the preparation of 4,13-diaza-18-crown-6 derivatives. The first was to prepare *N*,*N*′-dibenzyl-4,13-diaza-18-crown-6, remove the benzyl groups to afford the parent compound, and then alkylate with the incipient sidearm [27]. Alternately, the sidearmed macrocycle can be prepared in a single step. In this approach, a primary aliphatic amine, $R–NH_2$ in which R is the incipient sidearm, is treated with triethylene glycol diiodide in the presence of sodium carbonate and acetonitrile [29]. The latter approach is more direct and convenient. The former is lengthier but typically affords product in higher yield (Scheme 1).

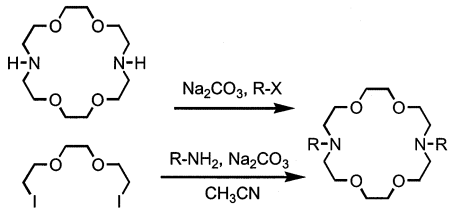

Scheme 1.

2.3. Cation binding studies

Solid-state data are important not only in providing details of the structure, but they also help the chemist to visualize the structural relationships. Solution data are important as well. They augment and confirm the solid-state data and they are a link with dynamic chemistry and reactions. During many years of study, we have assessed cation complexation strengths by use of ion selective electrodes, NMR, and calorimetric methods. Studies of compounds **4**–**6**, BiBLEs that have *n*-propyl, allyl, and propargyl sidearms, respectively, were conducted in methanol solution by using ion selective electrode techniques.

Comparisons of these molecules could be made directly because the ring size and sidearm length remained constant. Compounds **4**–**6** differ essentially in the extent of unsaturation. A perceived advantage of propargyl-sidearmed **6** over allyl derivative **5** was that the π-donors of **6** could exert their influence in any direction radiating from the π-cloud. In contrast, the π-bonds of the allyl sidearms must be appropriately oriented for a cation-π interaction to occur. This is illustrated in Fig. 8, which shows space-filling molecular models of butene and butyne as representatives of the sidearms of **5** and **6**. The cylindrical symmetry of the electron density of butyne is apparent in the structure on the right side of Fig. 8.

Previous studies of BiBLEs had clearly shown that sidearm participation could augment cation binding. The evidence for this was twofold. First, binding constants determined in methanol solution showed that when sidearm donor groups were positioned appropriately, ring complexation was augmented. An example is shown in Fig. 9. Two 15-crown-5 derivatives were prepared. In both cases, the sidearms were phenoxymethyl. To each arene was appended an additional methoxy group.

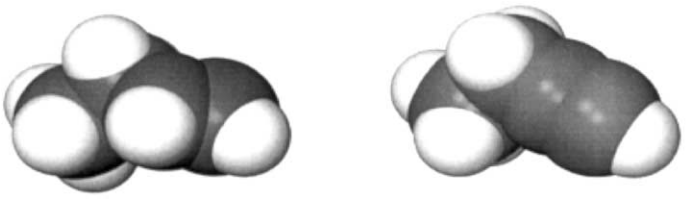

Fig. 8. Energy minimized structure of butene (left) and butyne shown in the CPK space-filling metaphor.

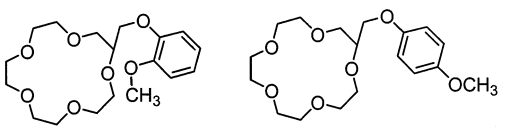

Ks (Na^+) = 1,740 Ks (Na^+) = 795

13 **14**

Fig. 9. Sodium cation binding by isomeric carbon-pivot lariat ethers.

Space-filling models showed that the phenoxymethyl oxygen atom was not positioned appropriately to enhance cation binding. When the complexation constants were measured in anhydrous methanol, the *o*-methoxy derivative had $\log K_S = 3.24$ and the corresponding value for the *p*-substituted analog was 2.90. Because crown ether complexation constant exhibit a broad range of values, they are usually expressed as the decadic log ($\log_{10}$). The corresponding equilibrium values are 1740 and 795 or more than a twofold difference due only to heteroatom donor group placement.

Binding constants ($\log K_S$) were measured for Na^+ at 25 °C in anhydrous methanol solution. The stability constants for the *n*-propyl (**4**), allyl (**5**), and propargyl (**6**) sidearmed BiBLEs were found to be: **4**, 2.86; **5**, 3.04; and **6**, 3.61. The values above translate to equilibrium binding constants of 725 (**4**); 1100 (**5**); and 4100 (**6**). These values are significant but they are well below the sodium cation binding constant reported in methanol for 18-crown-6: $\log K_S = 4.35$ ($K_S = 22\,400$) [32].

The observation that Na^+ binding strength increased with the level of unsaturation was encouraging and, indeed, it was the hoped-for result. Our initial interpretation was that sodium cation binding within the macroring was augmented by the π-systems present in the unsaturated sidearms. We were further encouraged in these studies by the observation that the K^+ binding constants exhibited a similar trend. Thus, experimentally determined $\log K_S$ values for K^+, again in anhydrous methanol solution, were as follows: **4**, 3.77; **5**, 4.04; and **6**, 4.99. Again, these values were lower than observed for 18-crown-6 binding K^+, $\log K_S$ for which is 6.08 ($K_S = 1.2 \times 10^6$). Interestingly, however, $\log K_S$ for **6** is only about a decade weaker binder than 18-crown-6.

2.4. Crystal structures of BiBLE compounds

Early in the study of lariat ethers, it proved essential to correlate solution binding results with solid-state structural data. A collaborative effort [33] was undertaken with Fronczek and Gandour that resulted in a number of crystal structures. These included free host molecules and various sidearmed complexes of Na^+ and K^+. It is worthwhile to consider how the sidearms participate in binding because the success of oxygen donors in the sidearms will be used as a model to attempt to observe similar interactions with π-donors.

Panels a and b of Fig. 10 show the solid-state structure of *N*,*N*′-dibenzyl-4,13-diaza-18-crown-6 (**15**) in ball and stick (a) and space-filling (b) metaphors. The six donors of the macrocycle participate in binding the cation and form an approximately equatorial belt about the cation. The apical positions are occupied by the SCN^- ion both above and below. The sidearms do not participate as donors in this complex and are turned away from the macrocycle-bound cation.

In contrast, *N*,*N*′-bis(2-methoxyethyl)-4,13-diaza-18-crown-6 (**16**) forms a complex with the K^+ cation that fully utilizes the sidearm oxygen donor atoms. In this particular case, complexation occurs from above and below although complexation of both sidearms on the same side of the macroring has been observed. The latter situation resembles the complexation geometry observed for cryptands.

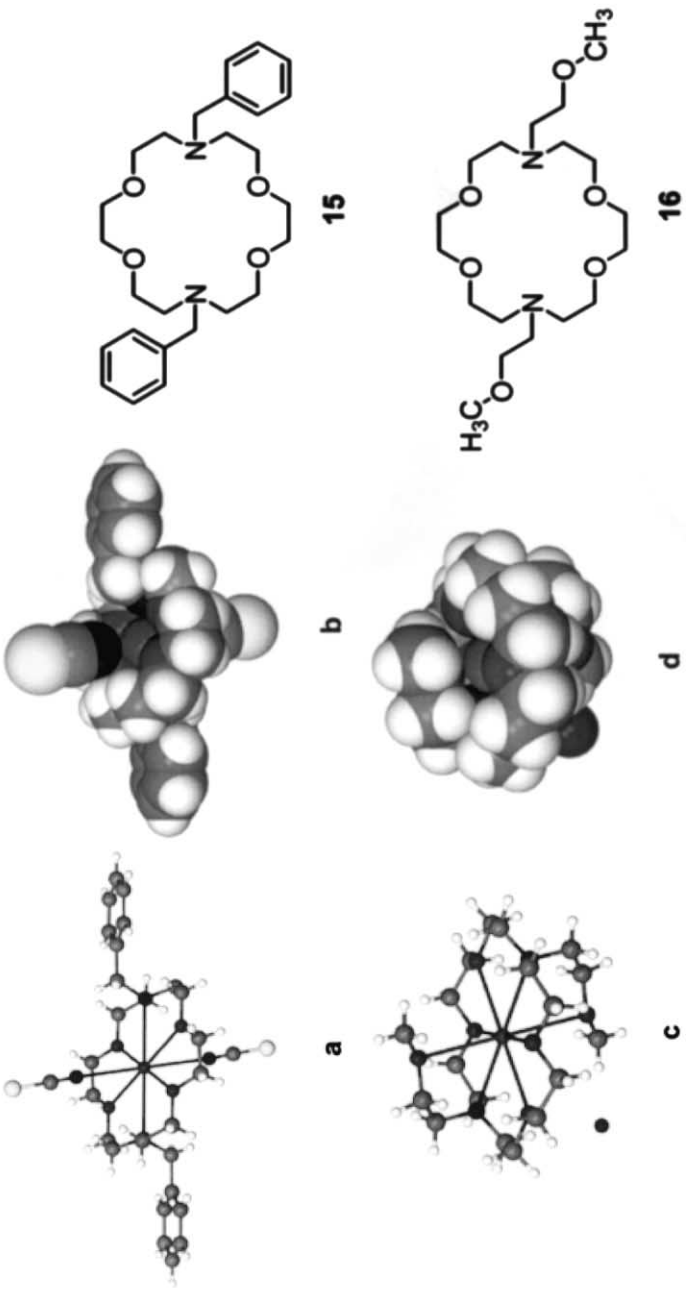

Fig. 10. Solid-state structures of **15** (panels a and b) and **16** (panels c and d).

In analogy to the structure observed for **16** · KI in which K^+ is fully enveloped, we hoped that **6** · KI would afford a complex in which the ring-bound cation was further complexed by the alkyne's triple bond electrons. A schematic illustration of the hoped-for complex is shown in Fig. 11. We did not rule out the possibility that sidearm participation could occur from the same side of the ring-bound cation in a cryptand-like arrangement. Thus, Fig. 11 shows a schematic of the anticipated *anti* structure for **6** · KI (panel a) and panel b shows the structure of *N*,*N*′-bis(2-hydroxyethyl)-4,13-diaza-18-crown-6, **17**, complexing KI. The structure of **17** · KI in which the sidearms are *syn* may be compared with the *anti* structure shown in Fig. 10 (panels c and d).

A substantial effort was undertaken to obtain crystals of **4**–**6** complexing cations. No sidearm participation in complexation was anticipated for *n*-propyl-sidearmed **4**, but hope was held for **5** and **6**, especially in light of the binding constant data. Two pictures of *N*,*N*′-bis(propargyl)-4,13-diaza-18-crown-6 complexing K^+ are shown in Fig. 12. The salt chosen for crystallization was KBF_4 because the tetrafluoroborate anion is regarded as nonnucleophilic. The anion was thus expected not to compete with the propargyl π-system making sidearm complexation as likely as possible. It is apparent from the figure that the sidearms do not interact with the ring-bound cation. Indeed they are rotated away from the macroring and are as remote from each other and the cation as possible. An interesting feature of

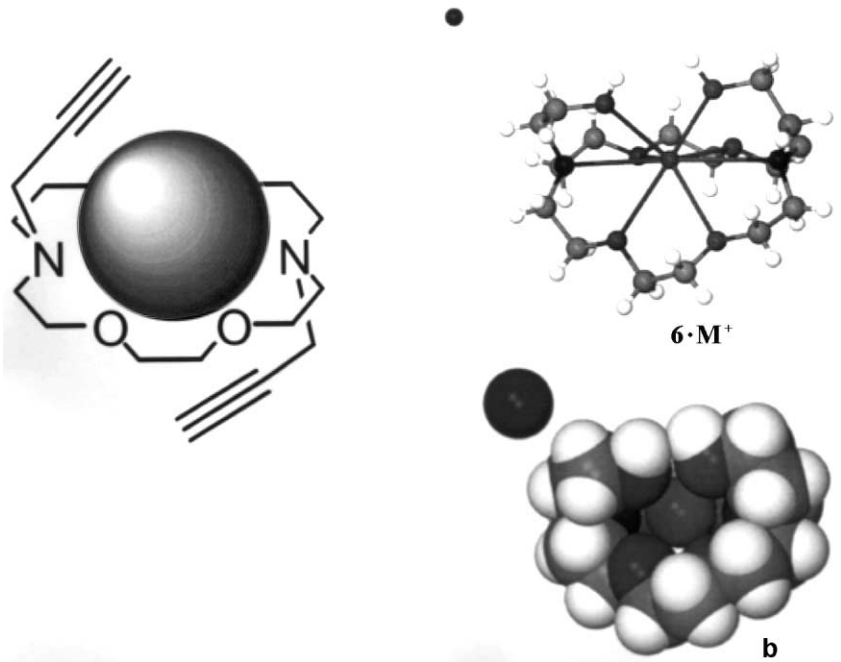

Fig. 11. Schematic representation of anticipated cation-π complexation by **6** (panel a) based on the known structure of *N*,*N*′-bis(2-hydroxyethyl)-4,13-diaza-18-crown-6 (panel b).

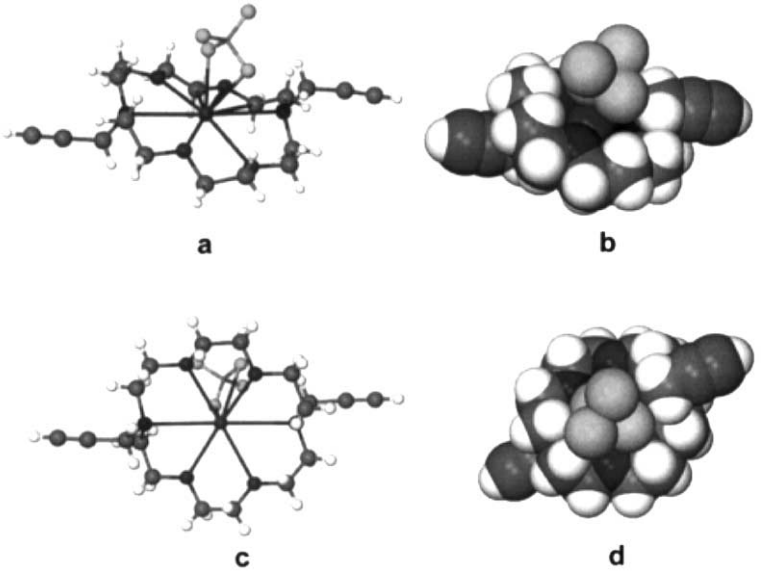

Fig. 12. Solid-state structures of **6** in ball and stick (panel a) and space-filling (panel b, same view as panel a) representations. Panels c and d are bottom and top views, respectively, of the complex shown in ball and stick and space-filling representations.

the structure is that the 'nonnucleophilic' fluorines are interacting directly with the cation as the apical substituent. Potassium is bonded to two of the four fluorines, which are at distances of ~ 2.7 and 3.4 Å from it. Panels a and b of Fig. 12 are the same view of the structure shown in ball and stick and CPK representations, respectively. Bottom (panel c) and top (panel d) views are also shown to clarify the position of the cation within the macroring and the counterion.

The crystal structure evidence seemed to be at odds with the solution binding data. Solid-state structures clearly represent an energy minimum and are, by their very nature, valid conformations. Still, the combination of packing forces in the solid and solvation forces in solution could lead to a predominance of one or the other. It was therefore decided to carry the solution studies further to see if useful thermodynamic data could be obtained.

2.5. Determination of binding thermodynamics

Izatt, Christensen, and their coworkers had obtained a mass of thermodynamic data for a variety of complexing agents and cations [6,34]. We felt that this database could provide calibration for the interactions we observed. We also thought thermodynamic data would reveal whether or not there was an increase in the enthalpic contribution to binding as the extent of sidearm unsaturation increased. We had previously obtained acceptable thermodynamic data using the so-called van't Hoff isochore or van't Hoff equation: [35] $\mathrm{d} \ln K/\mathrm{d}T = \Delta H/R\mathrm{T}^2$. A

plot of ln K_S versus $1/T$ (K) gives a line having a slope of $\Delta H/R$ and an intercept of $\Delta S/R$. Typically, the log of the equilibrium constant is plotted versus inverse temperature (abscissa). The equilibrium binding constant is determined for a range of temperatures. The temperatures selected depend on the reaction but a convenient range for the present studies was 15–41 °C.

The data obtained by using the van't Hoff method are recorded in Table 2 for compounds **4**–**7**. Compound **7** is isosteric with propargyl derivative **6** but the triple bonds of **7** are terminated by nitrogen (–CH_2≡CN:). The presence of nitrogen also influences polarity and the ability of the sidearm to serve as an electron donor or as an H-bond acceptor.

We had been encouraged by the apparently linear increase in log K_S for **4**–**6** with increasing unsaturation. Some of the data shown in Table 2 have been graphed in Fig. 13. The data are fit by straight lines with a confidence factor r^2 of $>90\%$ in both cases. Of course, this is far from excellent for three points but the trend was strongly suggestive. A determination of the binding constant for **7**, the sidearm of

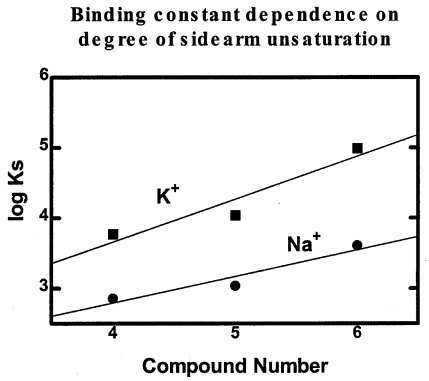

Fig. 13. Graph showing the increase in K_S with increasing unsaturation for compounds **4**–**6**.

Table 2
Equilibrium constants and thermodynamics of cation binding affinities

No.	Sidearm	log K_S		Sodium cation		Potassium cation	
		Na^+	K^+	ΔH	$T\Delta S$	ΔH	$T\Delta S$
–	18-Crown-6	4.34	6.09	-7.40 ± 0.11	-1.50 ± 0.09	-11.3 ± 0.02	-3.03 ± 0.04
4	$CH_2CH_2CH_3$	2.86	3.77	-2.82 ± 0.05	1.08 ± 0.04	-6.28 ± 0.27	-1.14 ± 0.30
5	$CH_2CH{=}CH_2$	3.04	4.04	-3.56 ± 0.23	0.59 ± 0.20	-7.34 ± 0.02	-1.84 ± 0.01
6	CH_2–C≡CH	3.61	4.99	-4.97 ± 0.04	-0.05 ± 0.12	-4.97 ± 0.04	-0.05 ± 0.12
7	CH_2–C≡N:	2.69	3.91	-4.87 ± 0.08	-1.20 ± 0.10	-9.54 ± 0.11	-4.21 ± 0.09
–	$CH_2CH_2OCH_3$	4.77	5.52	-7.20 ± 0.05	-0.73 ± 0.08	-8.81 ± 0.03	-1.28 ± 0.02

Values determined in CH_3OH (anhydrous) at 15–41 °C as described in Ref. [28]. log K_S values in M^{-1}, enthalpy values in kcal mol^{-1}; entropies in e.u.

which is the same size and shape as that of **6**, showed lower binding values for both Na^+ and K^+. This was clearly concerning. Of greater importance was the finding that ΔH for sodium binding with either **6** or **7** was about the same (~ 4.9 kcal mol^{-1}) but substantially different for K^+ binding (4.97 vs. 9.54 kcal mol^{-1}). We felt this could only mean that forces different from cation-π interactions must be at work. Taken together with the unsuccessful attempt to obtain solid-state evidence for cation-π interactions, the effort was abandoned for a number of years (Fig. 13).

3. Cation channels and cation-π interactions

Natural proteins that conduct cations present an interesting problem to the chemists. If protein channels are visualized as being tube-like structures constructed from transmembrane α-helices, one can imagine Na^+ selectivity resulting from the size of the pore. Smaller cations could pass through but Na^+ is so much more abundant than Li^+ or Mg^{2+} that there would be little reason for selectivity. One can invoke electronic and solvation criteria to account for Ca^{2+} versus Na^+ selectivity, even though the cations are almost identical in ionic radius. It is more difficult to account for K^+-channel selectivity on the basis of size. Clearly, K^+ (diameter = 2.66 Å) is larger than Na^+ (diameter = 1.98 Å). While larger K^+ cannot pass through a 'sodium-sized' pore, there is no steric reason why Na^+ could not freely pass through a pore large enough for K^+.

As noted above, Dougherty and coworkers advanced a theory to account for K^+ selectivity that was based on cation-π interactions involving amino acid sidechains. The theory will not be recounted here. Suffice it to say that the hypothesis could be tested experimentally. MacKinnon and coworkers, a leading group of channel biophysicists, did this. Site directed mutagenesis was used to alter a tyrosine residue (to phenylalanine) in the putative selectivity filter of a K^+-selective channel [5]. Potassium selectivity was lost in the mutagenized channel, even though an arene was still present in the same position. The cation-π hypothesis was thus discounted. Still, these efforts stimulated interest in alkali metal cation-π interactions. Our efforts to develop a synthetic cation channel [36] were underway at that time and this controversy rekindled our interest in obtaining experimental evidence for cation-π interactions.

4. Aromatic sidearms of amino acids

It occurred belatedly to us that the absence of olefins and alkynes in the sidechains of the 20 common protein amino acids was not coincidental. If significantly stabilizing interactions were possible that involved olefins, it seemed reasonable to think that evolution would have used this circumstance to advantage. There are, however, four protein amino acids that possess aromatic sidechains. Three of

them were identified above as Phe, Tyr, and Trp. A fourth example is histidine; imidazole terminates its sidechain. To be sure, imidazole is aromatic but its chemistry is dominated by the ring nitrogen atoms that are σ-donors. We thus focused our attention on Phe, Tyr, and Trp in designing receptor systems to probe cation-π interactions.

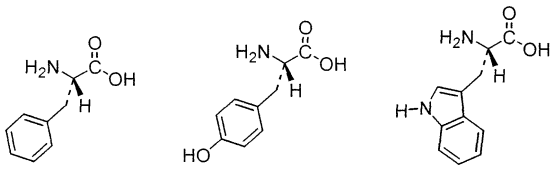

A feature of these three amino acids that we had not previously considered struck us. In each case, the arene was connected to the nitrogen atom by two carbons. We already knew from solution binding and solid-state studies (see above) that *N*,*N*′-dibenzyl-4,13-diaza-18-crown-6 showed no evidence of cation-π interactions. The benzene ring is attached to the macroring nitrogen atom by a single carbon. If we were to be guided by the amino acid, the target receptor molecule would be *N*,*N*′-bis(2-phenylethyl)-4,13-diaza-18-crown-6.

We prepared molecular models of compounds **9**–**11**. The increased flexibility of the sidechains conferred upon them by the presence of an additional carbon atom was apparent. Indeed, Monte Carlo simulations conducted on the 2-arylethyl-substituted diaza-18-crown-6 derivatives suggested that the sidearms enjoyed ample flexibility. The appropriate extension of the sidearm aryl donor group to the bound

Fig. 14. Monte Carlo conformational search conducted on **11** in which one indolylethyl sidearm was held in a fixed position.

cation's apical position was also apparent from an examination of models. Fig. 14 shows the calculated conformations of **11**. The lower indolylethyl sidearm was held fixed and the upper arm was allowed to adopt all conformations within a 10 kcal energy window.

An additional issue that was of concern in the design of receptor molecules related to Phe, Tyr, and Trp concerns the latter. Theoretical studies all suggested that the benzene ring of indole would be a better (stronger) π-donor than would be the pyrrole ring. Fig. 15 shows the results of calculations obtained with the commercially available SPARTAN 5 program. The electrostatic surfaces show areas that are relatively more negative as red and those that are more positive are shown in blue. The numbers shown are calculated, gas phase donicities in kcal mol^{-1}.

We carefully examined the molecular models of **11** and its Na^+ and K^+ complexes to be certain that the benzene ring could easily position itself over the ring-bound cation. The two-carbon sidechains were sufficient for the benzene and phenol substituents to overreach the bound cation's apical positions and we assumed that, if successful, the arenes would be positioned to maximize stability. Of course, this was expected in the case of **11** but we did not wish foreseeable steric constraints to determine the position of interaction.

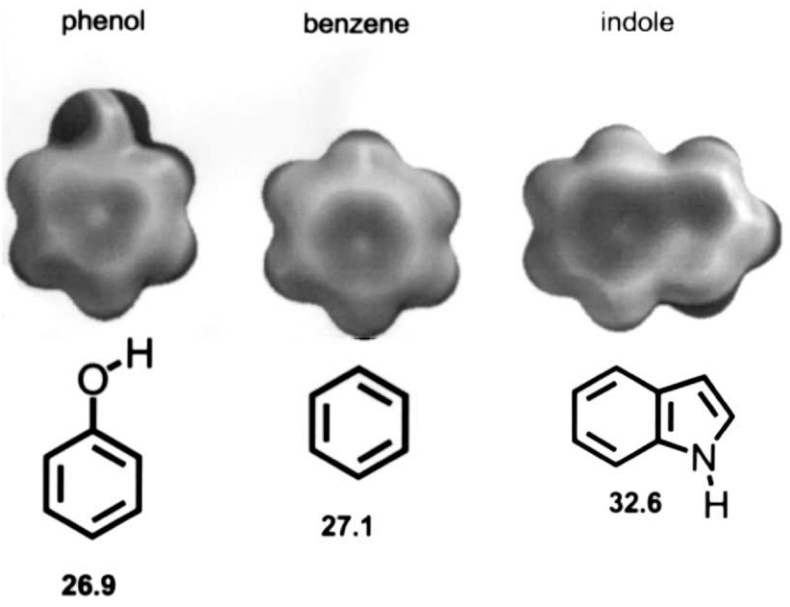

Fig. 15. Gas-phase electrostatic potential surfaces and stabilization energies for benzene, phenol, and indole.

5. Solid-state structures demonstrating alkali metal cation-π interactions

The three compounds that were the principal targets of the present studies were compounds **9**–**11**. Their structures are shown above. They are diaza-18-crown-6 derivatives having benzene, phenol, or indole attached at the end of a two-carbon chain. Phenol and indole are attached in their 4- and 3-positions, respectively, as they are in the natural amino acids. Each receptor was dissolved in an organic solvent, typically acetone, along with a sodium or potassium salt. Most experimental attempts were made with either NaI or KI and complexes suitable for X-ray analysis were obtained in a number of cases.

5.1. The indole-substituted receptor, ***11***

Computational studies suggested that among the three arenes, indole should be the best π-donor for alkali metal cations (see Fig. 15). Crystals were isolated and solid-state structures were obtained. Fig. 16 shows the solid-state structure of **11** · KI [37]. It is apparent from the ball and stick representation that the potassium cation is in the center of the macrocyclic ring. Each of the sidearms is extended up and over the ring-bound cation and the arenes are close enough to interact strongly with K^+.

The enveloping nature of the complex is more apparent in the CPK representation. Except for the presentation, the two views are identical. In the CPK format, it is apparent that not only are the arenes positioned above and below the ring-bound cation, but K^+ is fully isolated from the iodide anion (the sphere near the upper left). Iodide, of course, has a full negative charge and should be very effective in solvating the cation. Instead, the pair of indoles that serve as π-donors supplants it. It should also be noted that the iodide anion is stabilized by a NH···I hydrogen bond with one of the indole residues.

A similar complex was isolated from **11** · NaI. Although the donor–metal distances were, as expected, shorter than in **11** · KI, the essential features of the

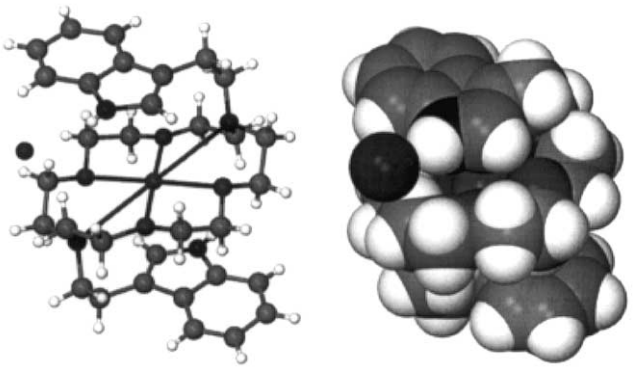

Fig. 16. Ball and stick and space-filling representations of the same view of the **11** · KI complex.

complex were identical. In particular, the closest contact between the ring-bound cation and the arene was near C2 of the pyrrole subunit rather than in the center of indole's benzene ring. In addition, iodide ion was excluded from sodium's coordination sphere and is H-bonded to one of the indole-NH groups.

It is interesting to compare the complexed and uncomplexed structures of **11**. This is done in Fig. 17. The free receptor adopts the typical 'parallelogram' conformation often observed for 18-crown-6 rings. Methylenes on opposite sides of the macroring turn inward to partially fill the internal void space. The sidearms are both turned away from the macrocycle. The ethylene chains that connect the arenes to the macrocycle are in the *anti* conformation.

The complex that forms between **11** and NaI is very similar to **11** · KI (see Fig. 16). In both cases, the pyrrole subunits of indole sandwich the alkali metal cation, which is bound within the 18-crown-6 macrocycle. In both cases, iodide is excluded from the solvation sphere and is H-bonded to an indole NH. When the structures of **11** · NaI and **11** · KI were first obtained, it was unclear why the pyrrolo- rather than the benzo-subunit was the preferred π-donor. This contravened the uniform results of computational studies and was surprising. We currently believe this to be a steric effect, a conclusion that is discussed further below.

5.2. The phenol-substituted receptor, ***10***

Compound **10** is related to tyrosine as **11** is related to tryptophan. The phenol residue terminates the crown's ethylene sidechain. Phenol is attached to the ethylene unit at the 4-position as it is in the amino acid. Fig. 18 (left) shows the solid-state structure of the unbound macrocycle in the ball and stick representation. Like the

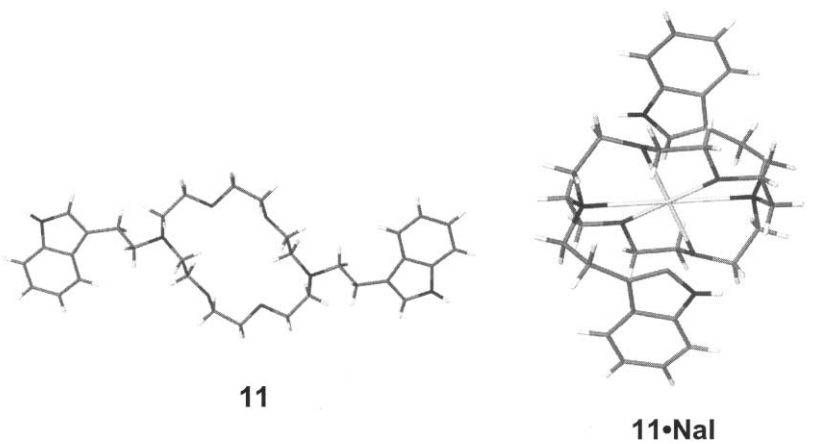

Fig. 17. Solid state structures of **11** (left) and **11** · NaI.

structure of free **11**, the macroring is in a parallelogram conformation. The two methylene groups of **10** that are turned inward on opposite sides of the macrocycle are somewhat more obvious than in the corresponding view of **11** shown in Fig. 17. As with **11**, however, the ethylene sidearms are in the *anti* conformation and they are turned away from the macrocycle. The phenol groups are as far away from each other as possible.

The complex **10** · KI is shown in a somewhat unusual representation. All of **10** is shown in the ball and stick representation but K^+ and I^- are illustrated in the space-filling metaphor. By using this mixed representation, it is easier to see the relationship between the phenol residues and the cation that they sandwich. As in the case of **11** · KI, the iodide ion is excluded from the solvation sphere and is H-bonded to one of the two phenolic hydroxyl groups. In the case of **10** · KI, K^+ is sandwiched almost exactly in the center of each benzene ring, in accord with theoretical predictions.

The structural similarities between the K^+ complexes of **10** and **11** are quite striking. In both complexes (**10** · KI and **11** · KI), all K^+–O distances fall within the

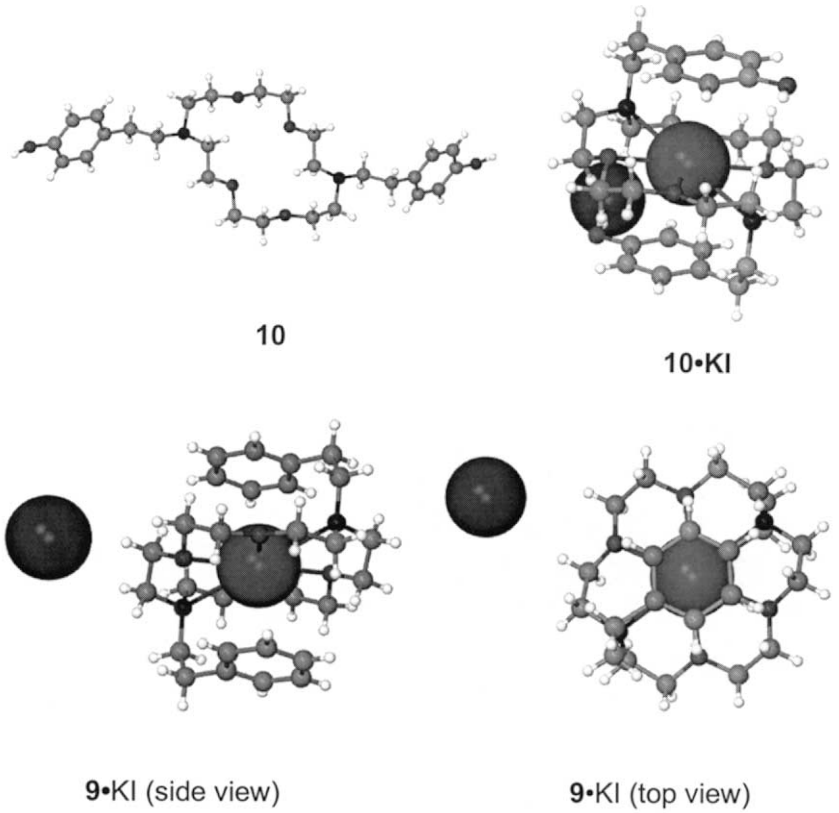

Fig. 18. (a) Structures of free **10** (left) and **10** · KI. (b) X-ray crystal structure of **9** · KI shown in side (left) and top views.

range 2.70 ± 0.06 Å. Likewise, the average K^+–N distance is 3.04 ± 0.01 Å. Even though K^+ is sandwiched by benzene rings in **10** and by pyrrole subunits in **11**, the K^+-centroid distance is 3.44 ± 0.01 Å for both complexes. The data are summarized in Table 3.

5.3. Benzene as a potential π-donor

The third of the three relevant aromatic amino acids is phenylalanine. Its arene is benzene and it possesses no H-bond donor that may interact with an iodide counter anion. Computational studies showed that benzene's π-donicity is essentially identical to that of phenol (see Fig. 15). It was feared that the absence of a hydrogen-bonding (H-bonding) donor to interact with iodide outside the complex might prevent the π-sandwich complex from forming. Association of the anion directly with the ring-bound cation is a well-known binding mode for crown ether complexes. If a direct interaction were favored between K^+ and I^-, the benzene rings would be unable to participate in the type of complexation observed for **10** and **11**.

N,*N*′-Bis(2-phenylethyl)-4,13-diaza-18-crown-6 (**9**) was prepared and found to have a melting point of 48–50 °C. Attempts to obtain crystals suitable for X-ray analysis failed, perhaps because of the low melting point. Good quality crystals of the KI complex were obtained and an X-ray structure was obtained. Two views of the structure are shown in Fig. 18. The figure on the left shows **9** · KI as viewed from the side and slightly above the center. The figure shows **9** in the ball and stick representation with the cation and anion in space-filling format. The sandwich complexation of K^+ is apparent. The position of the cation in the center of the arene is apparent from the top view shown at the right of the figure. It is very interesting to note that iodide is excluded from the complex even though there is no H-bond interaction to stabilize its position. Indeed, in a sense this observation was concerning as discussed in the next section.

Table 3
Comparison of bond distances for K^+ complexes of **10** and **11**

Complex	Interaction	Distance (Å)
10 · KI [a]	O–K average	2.70 ± 0.06
	N–K average	3.04
	K → centroid	3.44
11 · KI [b]	O–K average	2.70 ± 0.06
	N–K average	3.06
	K → centroid	3.45

[a] Data from Ref. [31].
[b] Data from Ref. [30].

5.4. Perfluorobenzene as a potential π-donor

Hexafluorobenzene and benzene are very similar in size. The carbon–carbon framework is identical and fluorine and hydrogen differ little in size. The van der Waals' radius of hydrogen is 1.20 Å and it is 1.35 Å for fluorine. The major difference is in electronegativity. Fluorine is strongly electron withdrawing relative to hydrogen so the π-center of hexafluorobenzene is far less electron rich than is benzene. Indeed, a SPARTAN 5 calculation showed that the center of perfluorobenzene is positive relative to benzene, which is negative.

Our observation that the complexes **9** · KI and **10** · KI were almost isosteric even though the former lacked any H-bond stabilization for the counter anion was troubling. It occurred to us that the observed π-stacking might arise from crystal packing forces and that it had little to do with the electronic issues. We therefore decided to exchange the benzene groups of **9** for pentafluorophenyl residues (→**18**). The structure of **18** is shown in Fig. 19 along with the X-ray crystal structure of the unbound receptor.

Unbound decafluoromacrocycle (**18**) is in the conformation expected. Presumably, this conformation is the same as would have been observed for **9**, had appropriate crystals been obtained. As with unbound **10** and **11**, the macrocycle is in a parallelogram arrangement and the sidearms are turned away from the macroring. The critical question is, of course, what happens when KI is complexed by this receptor? In principle, the macroring donors should be sufficient to stabilize K^+ to form a typical crown–cation complex. If a π-donor effect of the arene electrons, rather than crystal packing forces, determines the sidearm orientation, we expect the pentafluorophenyl sidearms to be turned away from the cation. If the sidearms do not coordinate the cation, interaction with adventitious water or directly with the iodide anion is expected. Indeed, as shown at the right of Fig. 19, the sidearms do not participate in complexation but the iodide ion does.

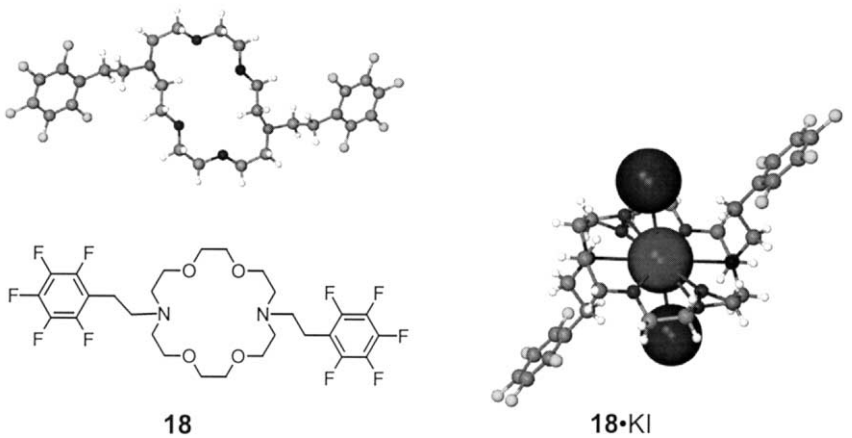

Fig. 19. Schematic and X-ray structures of **18**.

The single complex shown fails to fully convey the crystal arrangement that is observed. Two iodide ions are shown in Fig. 19 (right). Iodide and potassium form part of a continuous chain of stacked complexes. The macrocyclic rings would constitute a 'vertical channel' if the system were dynamic. Alas, it is not, and stacks of macrocycles are far removed from a functional cation channel.

The critical finding of this experiment is that the iodide complexes and neutralizes the ring-bound cation when the sidearms do not. This dispels the possibility that all of the apparent cation-π interactions that were previously observed result merely from crystal packing forces. The latter possibility was of less concern because solution NMR experiments showed that in acetone solution, **11** appeared to complex Na^+ in analogy to the solid-state structure.

5.5. An observation about steric effects

Computational studies predict that cation-π interactions will occur between alkali metal cations and benzene at or near the center of the π-system. In the complexes obtained for $\mathbf{9} \cdot M^+$ and $\mathbf{10} \cdot M^+$, this expectation was fully realized. The situation is more complicated for indole (**11**) because either the benzene or pyrrole subunit could serve as a π-donor. Theoretical studies uniformly identify the benzene ring as the π-donor. The solid-state complexes we have isolated in which cation-π interactions are in evidence invariably show proximity between the cation and pyrrole. We also noted a higher level of 'tilt' in the two sandwiching indoles than we observed for either benzene (**9**) or phenol (**10**). We have tentatively concluded that the pyrrole is preferred over benzene in this situation not because its π-donicity is greater but because it 'fits' better into the macrocycle cavity. Such a steric effect is potentially of great importance. A consideration of the computational data in the abstract would lead one to believe that only the benzene ring can complex an alkali metal. In fact, these experiments confirm that indole is far more versatile.

In proteins where the polarity is low and where water may be largely excluded, cation-π interactions are expected to be important. It is easy to imagine a situation in which tryptophan is positioned in such a way that it cannot interact by contact with benzene. The present results make clear that the pyrrole subunit presents a viable alternative to the benzene ring, making indole even more versatile than previously appreciated.

6. Conclusions

The experimental results presented here address the long-standing problem of characterizing alkali metal cation-π interactions. Unequivocal evidence has been obtained for alkali metal cation-π interactions between the arenes indole, phenol, and benzene. These are the three key aromatic residues on the amino acids tryptophan, tyrosine, and phenylalanine. The potential for cation-π interactions within proteins is substantial. These three amino acids comprise 8.4% of all known protein sequences. Thus, in a protein of moderate size, about 250 amino acids, there

could be as many as 21 cation-π contacts. These could be augmented by the H-bonding potential of both indole and tyrosine, neither of which appears to be diminished by simultaneous involvement in π-donor interactions.

Our original goal of demonstrating cation-π interactions between alkali metals and olefins and alkynes remains unfulfilled. To be sure, isolated double and triple bonds seem less biologically relevant than the arenes discussed here. Numerous cases of unsaturated fatty acids, phenyl groups, and unsaturated guest molecules are known in biology and should not be discounted. The double bonds of unsaturated fatty acids in membranes have generally been thought to affect membrane fluidity. Within the nonpolar insulating regime of a bilayer, cation-π interactions could be significant. Of course, the full scope of cation-π interactions that may occur in nature is currently in the most vague outline. Future studies in our laboratory and those of others will no doubt bring validation to these studies in particular and to this area of study in general.

Acknowledgements

We warmly thank the National Institutes of Health (GM 36262) and the National Science Foundation (CHE-9805840) for grants that supported this work. We are also grateful for an American Chemical Society Graduate Fellowship, funded by Procter and Gamble, to E.S.M.

References

[1] (a) C.J. Pedersen, J. Am. Chem. Soc. 89 (1967) 2495;
(b) C.J. Pedersen, J. Am. Chem. Soc. 89 (1967) 7077.
[2] (a) J.M. Lehn, J.P. Sauvage, J. Chem. Soc. Chem. Commun. (1971) 440;
(b) B. Dietrich, J.M. Lehn, J.P. Sauvage, Tetrahedron Lett. (1969) 2885.
[3] G. Gokel, Crown Ethers and Cryptands, Royal Society of Chemistry, Cambridge, 1990.
[4] R.A. Kumpf, D.A. Dougherty, Science 261 (1993) 1708.
[5] L. Heginbotham, Z. Lu, T. Abramson, R. MacKinnon, Biophys. J. 66 (1994) 1061.
[6] J. Sunner, K. Nishizawa, P. Kebarle, J. Phys. Chem. 85 (1981) 1814.
[7] B.C. Guo, J.W. Purnell, A.W. Castleman Jr., Chem. Phys. Lett. 168 (1990) 155.
[8] (a) O.M. Cabarcos, C.J. Weinheimer, J.M. Lisy, J. Chem. Phys. 110 (1999) 8429;
(b) O.M. Cabarcos, C.J. Weinheimer, J.M. Lisy, J. Chem. Phys. 108 (1998) 5151.
[9] (a) J. Wouters, Protein Sci. 7 (1987) 2472;
(b) B.T. King, B.C. Noll, Michl, J. Collect. Czech. Chem. Commun. 64 (1999) 1001.
[10] K. Hoffmann, E. Weiss, J. Organomet. Chem. 67 (1974) 221.
[11] D.C. Hrncir, R.D. Rogers, J.L. Atwood, J. Am. Chem. Soc. 103 (1981) 4277.
[12] G.W. Gokel, D.M. Dishong, C.J. Diamond, J. Chem. Soc. Chem. Commun. (1980) 1053.
[13] D.G. Stewart, D.Y. Waddan, E.T. Borrows, British Patent 785 229 filed 4 February 1955, published 23 October 1957.
[14] G.W. Gokel, S.H. Korzeniowski, Macrocyclic Polyether Syntheses, Springer, Berlin, 1982, 415pp.
[15] G.W. Liesegang, A. Vasquez, N. Purdie, E.M. Eyring, J. Am. Chem. Soc. 99 (1977) 3240.
[16] R.M. Izatt, J.S. Bradshaw, S.A. Nielsen, J.D. Lamb, J.J. Christensen, D. Sen, Chem. Rev. 85 (1985) 271.

[17] B.A. Moyer, in: G.W. Gokel (Ed.), Complexation and Transport. In: Molecular Recognition: Receptors for Cationic Guests, vol. 1, Elsevier Science, Oxford, 1996, pp. 377–416 (11 vols.).
[18] G.W. Gokel, J.E. Trafton, Cation Binding by Lariat Ethers, in: Y. Inoue, G.W. Gokel (Eds.), Cation Binding by Macrocycles, Marcel Dekker, New York, 1990, pp. 253–310.
[19] G.W. Gokel, in: J.L. Atwood, J.E.D. Davies, D.D. MacNicol (Eds.), Lariat Ethers. In: Inclusion Phenomena, vol. 4, Oxford University Press, Oxford, 1991, pp. 287–328.
[20] (a) V.J. Huber, S.N. Ivy, J. Lu, R.A. Bartsch, Chem. Commun. (1997) 1499;
(b) S. Katsuta, T. Kimura, Y. Kudo, R. Nakagawa, Y. Takeda, M.J. Ouchi, Inclusion Phenom. Mol. Recognit. Chem. 31 (1998) 89;
(c) K. Kita, T. Kida, Y. Nakatsuji, I. Ikeda, J. Chem. Soc. Perkin Trans. 1 22 (1998) 3857;
(d) R.A. Bartsch, H.-S. Hwang, V.S. Talanov, G.G. Talanova, D.W. Purkiss, R.D. Rogers, J. Org. Chem. 64 (1999) 5341.
[21] (a) J.S. McKechnie, M.G. Newton, I.C. Paul, J. Am. Chem. Soc. 89 (1967) 4819;
(b) P. Ganis, J.D. Dunitz, Helv. Chim. Acta 50 (1967) 2379;
(c) D.J. Robinson, C.H. Kennard, J. Chem. Soc. Chem. Commun. (1968) 914;
(d) D. Michel, W. Meiler, E. Angele, Z. Phys. Chem. (Leipzig) 255 (1974) 389 (Chem. Abstr. 81:119333).
[22] See: D.G. Bessarabov, J.P. Theron, R.D. Sanderson, Desalination 115 (1998) 279 (and references therein).
[23] (a) S. Mecozzi, A.P. West Jr., D.A. Dougherty, J. Am. Chem. Soc. 118 (1996) 2307;
(b) O. Donini, D.F. Weaver, J. Comput. Chem. 19 (1998) 1515.
[24] S.K. Burley, G.A. Petsko, FEBS 203 (1986) 139.
[25] P.C. Kearney, L.S. Mizoue, R.A. Kumpf, J.E. Forman, A. McKurdy, D.A. Dougherty, J. Am. Chem. Soc. 115 (1993) 9907.
[26] A. McCurdy, L. Jiminez, D.A. Stauffer, D.A. Dougherty, J. Am. Chem. Soc. 114 (1992) 10314.
[27] (a) V.J. Gatto, K.A. Arnold, A.M. Viscariello, S.R. Miller, G.W. Gokel, Tetrahedron Lett. (1986) 327;
(b) V.J. Gatto, K.A. Arnold, A.M. Viscariello, S.R. Miller, G.W. Gokel, J. Org. Chem. 51 (1986) 5373.
[28] K.A. Arnold, A.M. Viscariello, M.-S. Kim, R.A. Gandour, F.R. Fronczek, G.W. Gokel, Tetrahedron Lett. (1988) 3025.
[29] V.J. Gatto, G.W. Gokel, J. Am. Chem. Soc. 106 (1984) 8240.
[30] S.L. De Wall, L.J. Barbour, G.W. Gokel, J. Am. Chem. Soc. 121 (1999) 8405.
[31] S.L. De Wall, E.S. Meadows, L.J. Barbour, G.W. Gokel, J. Am. Chem. Soc. 121 (1999) 5613.
[32] D.M. Dishong, G.W. Gokel, J. Org. Chem. 47 (1982) 147.
[33] (a) F.R. Fronczek, V.J. Gatto, R.A. Schultz, S.J. Jungk, W.J. Colucci, R.D. Gandour, G.W. Gokel, J. Am. Chem. Soc. 105 (1983) 6717;
(b) F.R. Fronczek, V.J. Gatto, C. Minganti, R.A. Schultz, R.D. Gandour, G.W. Gokel, J. Am. Chem. Soc. 106 (1984) 7244;
(c) R.D. Gandour, F.R. Fronczek, V.J. Gatto, C. Minganti, R.A. Schultz, B.D. White, K.A. Arnold, D. Mazzochi, S.R. Miller, G.W. Gokel, J. Am. Chem. Soc. 108 (1986) 4078;
(d) S.R. Miller, T.P. Cleary, J.E. Trafton, C. Smeraglia, F.R. Fronczek, G.W. Gokel, J. Chem. Soc. Chem. Commun. (1989) 806.
[34] (a) R.M. Izatt, K. Pawlak, J.S. Bradshaw, R.L. Bruening, Chem. Rev. 91 (1991) 1721;
(b) R.M. Izatt, J.S. Bradshaw, K. Pawlak, R.L. Bruening, B.J. Tarbet, Chem. Rev. 92 (1992) 1261;
(c) X. Chen, R.M. Izatt, J.L. Oscarson, Chem. Rev. 94 (1994) 467;
(d) R.M. Izatt, K. Pawlak, J.S. Bradshaw, R.L. Bruening, Chem. Rev. 95 (1995) 2529.
[35] K.A. Arnold, L. Echgoyen, G.W. Gokel, J. Am. Chem. Soc. 109 (1987) 3713.
[36] G.W. Gokel, Chem. Commun. (2000) 1.
[37] All of the structures shown in this paper were created using X-Seed to manipulate the structural data and Pov-Ray to render the illustrations (X-Seed: L.J. Barbour, 1999; http://www.lbarbour.com/xseed/; Pov-Ray web site, http://www.povray.org).